

**Thick Target Yield Measurements for Proton Induced Reactions with
Mo, Co and Ni Elements in Havar Matrix for Proton
Activation Analysis of Steel Alloys**

A.Azzam^{1*}, A.A.Alharbi² and J.Alzahrany²

1- Nuclear Physics Dept., Nuclear Research Center, A.E.A, Cairo, Egypt

2 -Faculty of Sciences , Princess Nora Bint Abdul Rahman University, P.O. Box 226957 ,

Riyadh 11324, Saudi Arabia

Abstract. The thick target yields for the nuclear reactions $^{nat}\text{Ni}(p,x)^{57}\text{Ni}$, $^{nat}\text{Co}(p,x)^{58(m+g)}\text{Co}$ and $^{nat}\text{Mo}(p,x)^{95g,96(m+g)}\text{Tc}$ were measured, as a function of target thickness, using the thin foil activation technique with proton energy of 26.5 MeV. Havar material foils were used as a target, since it contains the ^{nat}Ni , ^{nat}Co , and ^{nat}Mo with accurately certified concentrations. The measured yields, as a function of target thicknesses were, measured for proton activation analysis purposes. Havar alloy was used, as a reference for the analysis of some steel samples or iron based matrices, since it has almost the same stopping power for the accelerated protons. The produced gamma activities in the target due to these nuclear reactions were estimated for the same purposes. The measured yield values were compared to some previously estimated values, when it was possible.

Keywords: Proton Activation / Thick target yield/ Havar alloy/ Mo/ Ni/ Co

* Author for correspondence: E-mail address: ahmedazzamus@gmail.com

1. Introduction

Proton activation analysis is a sensitive and non-destructive method based on inducing radioactivity in the target as result of nuclear reactions (Guerra, M.F., 2004). The main advantage of this method is its high accuracy even for very low concentrations. The origin of this advantage is the possibility of avoiding and removing contamination.

Moreover, PAA uses the properties of the nuclei of the elements, while classical methods use the properties of the electrons. Therefore, the measured analytical signal does not depend on the chemical state of the first element and is not sensitive to its chemical properties.

In addition, it is useful in the determination of surface concentrations in inhomogeneous solid materials, such as coated metals, due to the low range of charged particles (Shibata *et al.*, 1979 and Cojocarru *et al.*, 2003).

A quantitative and qualitative analysis for the materials components can be carried out using the PAA method, by irradiated the samples with appropriate protons, in order to produce an interaction with the nuclei of the selected elements and to generate a signal, specific to the element and quantitatively related to its concentration. During the irradiation period, nuclear reactions are produced, and then the radioactivity of radioisotopes produced during the irradiation time is measured. Thus, PAA can be used for the determination of the elemental composition for unknown samples.

When using the PAA analytical method, much care has to be devoted in order to, correctly take into account the proton induced production yield in the various layers of the alloy under analysis. In this study, we measured the thick target yields for some nuclear reactions induced by protons with incident energy of about (26.5 MeV) on some Havar alloy's elements, mainly Mo, Ni and Co as a function of target thickness. The cross sections of these reactions were studied, by several authors (Zweit *et al.*, 1993; Takaces *et al.* 2003 ; Al-Saleh *et al.*,2006; Khandaker *et al.*, 2007; Alharbi *et al.*,2011 and Kandaker *et al.*,2011), from which the integral yield could be estimated. The self-absorption of the emitted gamma rays reduces the measured yield values in comparison with the estimated ones. Therefore thick target yield measurements are essential for proton activation analytical methods. The study will help in deriving the most suitable parameters for analyzing the above-mentioned elements in some Havar similar alloys.

2. Experimental technique.

The elemental proton induced reaction thick target yields (TTY) on some elements of the Havar alloy target were measured. The studied nuclear reactions are ${}^{\text{nat}}\text{Ni}(p,x){}^{57}\text{Ni}$, ${}^{\text{nat}}\text{Co}(p,x){}^{58(\text{m}+g)}\text{Co}$ and ${}^{\text{nat}}\text{Mo}(p,x){}^{95g,96(\text{m}+g)}\text{Tc}$. The activation method

and the well established stacked foil technique combined with high resolution gamma-ray spectroscopy was used (Alharbi et al.,2011).

2.1 Discription of target and irradiation.

Havar alloy is a heat treatable cobalt-based alloy that provides very high strength, with known typical composition of: Be 400 ppm, Cobalt 42.0%, Molybdenum 2.2%, Chromium 19.5%, Manganese 1.6%, Nickel 12.7%, Carbon 0.2%, Tungsten 2.7% and Iron 19.1%. The average density is 8.3 g/cm³. Table 1 contains the most important elements in HAVER material with their existing ratios, as given by the supplier, and natural isotopic compositions (Fireston et al., 1998)

Table (1): The most important elements in HAVER material with their existing ratios after ESPI Metals (Ashland, Oregon, US) and natural isotopic compositions (Fireston et al., 1998).

<i>Elements</i>	<i>z</i>	ρ ₃ (g/cm ³)	<i>isotopes</i>	<i>abundance</i>	<i>ratio in Havar %</i>
Cobalt	27	8.83	⁵⁹ Co	100	42.0
Chromium	24	7.19	⁵² Cr ⁵³ Cr ⁵⁴ Cr	83.79 9.50 2.36	19.5
Nickel	28	8.85	⁵⁸ Ni ⁶⁰ Ni ⁶¹ Ni ⁶² Ni	68.08 26.1 1.13 3.59	12.7
Tungsten	74	19.3	¹⁸² W ¹⁸⁴ W ¹⁸⁶ W	26.3 30.7 28.6	2.7
Molybdenum	42	10.23	⁹⁴ Mo ⁹⁵ Mo ⁹⁶ Mo ⁹⁷ Mo ⁹⁸ Mo	9.3 15.9 16.7 9.6 24.1	2.2

<i>Elements</i>	<i>z</i>	ρ ₃ (g/cm ³)	<i>isotopes</i>	<i>abundance</i>	<i>ratio in Havar %</i>
Manganese	25	7.44	⁵⁵ Mn	100	1.6
Carbon	6	2.25	¹² C	98.89	0.2
Iron	26	7.86	⁵⁴ Fe ⁵⁶ Fe ⁵⁷ Fe ⁵⁸ Fe	5.8 91.8 2.15 0.29	19.1

ESPI Metals (Ashland, Oregon, US) provided Havar foils as a sheet of 27 μm thickness, which was prepared as discs of 10 mm diameter. The foils were irradiated, in a form of stack, in an Al target holder which was described in a previous work (Alharbi et al.,2011). To confirm the cyclotron beam intensity and energy, a thin copper monitor foil (50 μm) of high-purity 99.999%, supplied by (Goodfellow, Cambridge, UK), was placed in front of the stack and irradiated in the same condition as the target (Al-Saleh et al.,2006). The degradation of the incident proton energy when passing through the foils was calculated using a computer program STOPING, for multi elemental target based on the stopping energy values of protons in the different materials (Ziegler et al., 1985). A number of 50 foils, with total thickness of 1350 μm were found to be enough to stop completely the incident protons. Irradiations were performed on the stack for 20 minutes using external beam of 100 nA protons with energy of about 26.5 MeV provided by TCC CS-30 Cyclotron at king Faisal Hospital & Research centre KFSH&RC in Riyadh, Saudi Arabia. This cyclotron is an isochronous azimuthally varying field, medium size and single energy one (Barrall et al., 1983). The proton energy was degraded from 26.5 to 25.9 MeV on passing the Cu faille. The average energy in the middle of the foil was found to be 25.22 MeV.

2.2 Activity measurements:

After irradiation the target holder with the foils were left for about 60 minutes to reduce the background activity, then dismantled and divided to 17 groups, each of three foils of total thickness of 81 μm. The average energy in the middle of each group were calculated and listed in table 4. The energy degradation varied gradually from 0.98, at incidence, to 3.2 MeV at the end of the range .The activities of the foils were measured in an accumulated sequence to increase the target thickness ranging from 81 to 1350 μm in 81 μm steps, using HPGe detector of intensity (50% relative to 3x3" NaI(Tl) detector) and the necessary electronics. The

spectrometer energy resolution was 2.2 keV for the 1.332 MeV γ -line of the ^{60}Co standard source, a peak-to-Compton ratio of 58: 1. In general, the activities of the samples were measured at a target-detector distance of 20 cm while looking for the longer-lived products, and between 20 and 55 cm in case of shorter-lived products to keep the dead time within 6%. The decay data of all investigated radionuclides were taken from the table of isotopes (Fireston et al., 1998). The produced yield (non corrected for self absorption) was calculated using the well-known formula (1) Bondardi, M (1988).;

$$Y_{integrated} \left(\frac{Bq}{\mu A.h} \right) = \frac{\lambda T_{\gamma}}{\epsilon_{abs} I_{\gamma} I C e^{-\lambda t_c} (1 - e^{-\lambda t_m}) t_b} \quad (1)$$

Where: λ is the decay constant of the produced isotope, T_{γ} is the area under the photo peak, ϵ_{abs} is the absolute detector efficiency, I_{γ} is the absolute intensity of the gamma line, I is the beam intensity in μA , C is the percentage of the element in the target, t_c is cooling time, t_m is the measuring time, and t_b is the irradiation time.

3. Results and discussions

The degradation of the proton energy through the target was found to be very similar to that through some iron-based target containing some impurities. Therefore, the Haver material can be fairly used as a standard material for steel samples. Some proton induced nuclear reaction reactions on some isotopes of Mo, Co and Ni were used to identify the existence of these elements in the Haver material. The used nuclear reactions for identifications are listed, along with their nuclear data, in Table 2. The most important interfering reactions with their threshold energies (www.nndc.bnl.gov/qcalc/qcalc.jsp.) and decay data are presented in Table 3.

Table (2): The used Nuclear reactions along with their most important nuclear data (Fireston et al., 1998) .

Element to be determined	Principal reactions	Isotopic abundance %	Q-value MeV	Half life	Decay mode	E_{γ} keV	I_{γ} %
Ni	$^{58}\text{Ni}(p,pn)^{57}\text{Ni}$	68.08	-12.22	35.6h	EC(60) β^+ (40)	127.164	16.7
	$^{60}\text{Ni}(p,nt)^{57}\text{Ni}$	26.16	-24.12			1377.63 1919.52	81.7 12.25
Co	$^{59}\text{Co}(p,pn)^{58g}\text{Co}$	100	-10.45	70.82 d	EC+ β^+	810.76	99.4
	$^{59}\text{Co}(p,pn)^{58m}\text{Co}$			9.15 h			

Element to be determined	Principal reactions	Isotopic abundance %	Q-value MeV	Half life	Decay mode	E_γ keV	I_γ %
Mo	$^{95}\text{Mo}(p,n)^{95g}\text{Tc}$	15.9	-2.47	20 h	EC	765.79	93.82
	$^{96}\text{Mo}(p,2n)^{95g}\text{Tc}$	16.7	-11.63			947.67	1.95
	$^{97}\text{Mo}(p,3n)^{95g}\text{Tc}$	9.6	-18.45			1073.71	3.74
	$^{96}\text{Mo}(p,n)^{96g}\text{Tc}$	16.7	-3.76	4.28 d 51.5 m	EC+ β^+ IT(98)	778.22	99.76
	$^{96}\text{Mo}(p,n)^{96m}\text{Tc}$					812.58	82.0
	$^{97}\text{Mo}(p,2n)^{96g}\text{Tc}$	9.6	-10.58			849.92	98.0
	$^{97}\text{Mo}(p,2n)^{96m}\text{Tc}$						
	$^{98}\text{Mo}(p,3n)^{96g}\text{Tc}$	24.1	-19.22			778.22	1.9
	$^{98}\text{Mo}(p,3n)^{96m}\text{Tc}$					1200	1.08

Table (3): The interfering nuclear reactions with their nuclear data (Fireston et al., 1998).

Element to be determined	Activation reaction used	E_{thr} MeV	Interfering reaction	E_{thr} MeV
Ni	$^{58}\text{Ni}(p,pn)^{57}\text{Ni}$	12.43	$^{59}\text{Co}(p,3n)^{57}\text{Ni}$	23.5
	$^{60}\text{Ni}(p,nt)^{57}\text{Ni}$	24.5		
Co	$^{59}\text{Co}(p,pn)^{58}\text{Co}$	10.6	$^{58}\text{Fe}(p,n)^{58}\text{Co}$	3.1
			$^{60}\text{Ni}(p,2pn)^{58}\text{Co}$	20.3
			$^{61}\text{Ni}(p,2d)^{58}\text{Co}$	23.7
			$^{62}\text{Ni}(p,\alpha n)^{58}\text{Co}$	10.3
			$^{64}\text{Ni}(p,3n\alpha)^{58}\text{Co}$	27

3.1 Thick target yields (TTY)

The non correcter thick target yield for the nuclear reactions $^{nat}\text{Ni}(p,X)^{57}\text{Ni}$, $^{nat}\text{Co}(p,X)^{58(m+g)}\text{Co}$, $^{nat}\text{Mo}(p,xn)^{95g}\text{Tc}$ and $^{nat}\text{Mo}(p,xn)^{96(m+g)}\text{Tc}$ were measured as a function of the proton energies and hence the target thickness, to the first time during this work, using the degradation of the 25.9 MeV proton beam through the target foils. It is noticed that the entire measured yield were not corrected, even it is not stated in the text.

3.2. Thick target yield of $^{nat}\text{Co}(p,X)^{58(m+g)}\text{Co}$

The thick target yield of the reaction $^{nat}\text{Co}(p,X)^{58(m+g)}\text{Co}$ was measured as a function of the target thickness and presented in Fig.1. The proton energy decreases due to the degradation in the target and completely absorbed at a thickness of about 1300 μm . The measured yield values increase gradually with the target thickness until about 900 μm and then starts to saturate at a value of about 7 MBq/ μAh . The proton energy at this thickness is about 14 MeV, which is close to the threshold energy of the $^{59}\text{Co}(p,pn)$ reaction producing $^{58(m+g)}\text{Co}$ isotope at 10.6 MeV. The measured yield values along with the target thickness and proton energies are listed in table 4.

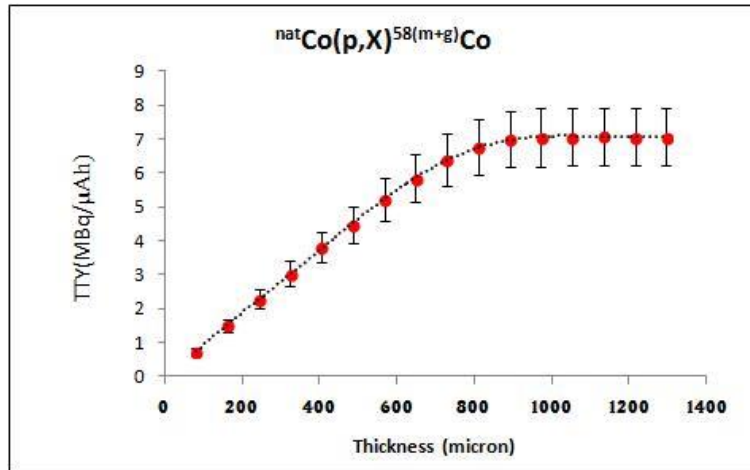


Fig.1: measured non corrected thick target yield (TTY) of $^{nat}\text{Co}(p,X)^{58(m+g)}\text{Co}$ nuclear reaction as a function of Haver target thickness for $E_p = 25.5$ MeV.

In order to use this data in practical elemental analyses, the activity due to the production of ^{58}Co isotope, from ^{nat}Co , per unit surface density in the target (m_i) was calculated, noticed as a normalization value, and plotted as a function of the target thickness in Fig.2. The measured activity was about 11 ((MBq/ μAh)/(g/ cm^2)) and was almost constant in the thickness range from 80 to 800 μm and decreases gradually at larger thickness, as given in table 5. The result shows that this reaction is suitable for measuring the Co concentration in surface thickness of about 800 μm or less.

Table: (4). Measured yield values corresponding to proton energies and related target thickness for different proton induced reactions.

No. of Foil	Thickness (µm)	Energy range from 25.9 MeV to	Thick target yield (MBq/µAh)			
			^{nat} Co(p,x) ^{58(m+g)} C _o	^{nat} Ni(p,x) ⁵⁷ Ni	^{nat} Mo(p,xn) ^{95g} T _c	^{nat} Mo(p,xn) ^{96(m+g)} T _c
1-3	81	25.22	0.74 ± 0.09	12.07±1.44	10.95±1.31	2.74±0.33
1-6	162	24.27	1.50 ± 0.18	23.35±2.80	16.80±2.02	5.06±0.61
1-9	243	23.29	2.27 ± 0.27	33.89±4.06	29.88±3.59	7.09±0.85
1-12	324	22.27	3.04 ± 0.36	43.44±5.21	34.985±4.19	8.32±0.99
1-15	405	21.22	3.80 ± 0.46	49.04±5.88	42.82±5.14	10.14±1.22
1-18	486	20.12	4.49±0.54	61.85±7.42	51.34±6.16	11.97±1.44
1-21	567	18.98	5.21±0.63	73.46±8.81	64.015±7.68	14.63±1.76
1-24	648	17.79	5.85±0.7	76.28±9.15	79.289±9.52	16.16±1.94
1-27	729	16.53	6.40±0.77	79.96±9.59	86.127±10.34	17.27±2.07
1-30	810	15.12	6.78±0.81	82.85±9.94	84.423±10.13	18.92±2.27
1-33	891	13.77	7.00±0.84	84.16±10.1	92.565±11.11	20.96±2.52
1-36	972	12.23	7.05±0.85	83.69±10.04	103.63±12.44	22.67±2.72
1-39	1053	10.52	7.06±0.85	83.5±10.02	108.15±12.98	26.32±3.16
1-42	1134	8.59	7.08±0.85	83.84±10.06	121.67±14.60	26.92±3.23
1-45	1215	6.28	7.07±0.85	83.40±10.01	113.73±13.65	27.88±3.35
1-48	1296	3.07	7.06±0.85	82.73±9.92	118.81±14.26	27.43±3.29

The concentration of any element, in steel like samples, could be estimated using the following equation:

$$C_i = A_i / m_i \tag{2}$$

Where, C_i is the concentration of the ith element in units of g/cm².

A_i is Activity of the mentioned isotope in the element i .

m_i is the normalization factor for the element i .

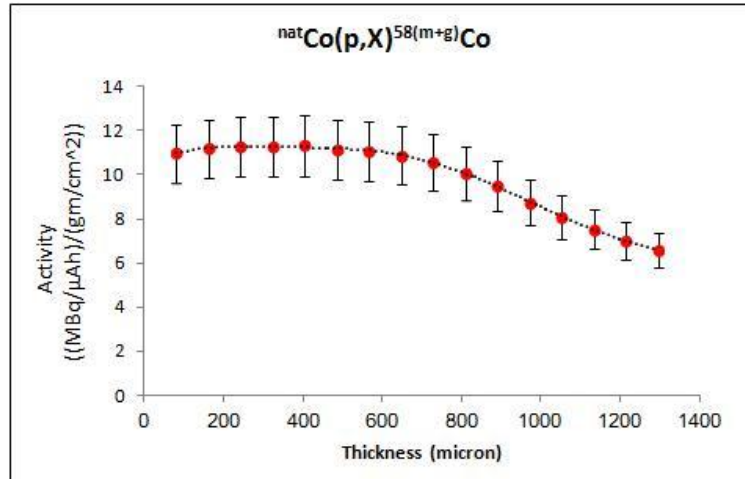


Fig. 2: $^{58(m+g)}\text{Co}$ activity (normalization value m_i) as a function of Co surface density in Haver target.

3.3 Thick target yield of $^{nat}\text{Ni}(p,X)^{57}\text{Ni}$

Fig.3 indicates the measured thick target yield for the reaction $^{nat}\text{Ni}(p,X)^{57}\text{Ni}$ as a function of the Haver target thickness. The produced yield is mainly due to the reaction (p,pn) on ^{58}Ni . It is shown from the figure that, there exists a linear increase of the yield with the target thickness up to about 730 μm . A saturation value of about 80 $\text{MBq}/\mu\text{Ah}$ was observed for thicknesses larger than 800 μm , which is corresponding to proton energy of about 15 MeV. The measured yield values along with the target thicknesses and proton energies are listed in table 4. The activity due to the production of ^{57}Ni isotope per unit surface density in the target (m_i) was calculated from the yield values and found to fluctuate between 160 and 180 $((\text{MBq}/\mu\text{Ah})/(\text{gm}/\text{cm}^2))$ up to target thickness of about 650 microns, as seen in table 5.

Table (5): normalization values (m_i), corresponding to proton energies and related target thickness for different proton induced reactions.

No.of Foil	Thickness (μm)	Energy (MeV)	Activity $\{(\text{MBq}/\mu\text{Ah})/(\text{gm}/\text{cm}^2)\}$ (m_i)			
			$^{nat}\text{Co}(p,x)^{58(m+g)}\text{Co}$	$^{nat}\text{Ni}(p,x)^{57}\text{Ni}$	$^{nat}\text{Mo}(p,xn)^{95g}\text{Tc}$	$^{nat}\text{Mo}(p,xn)^{96(m+g)}\text{Tc}$
1-3	81	25.22	10.98 ± 1.32	179.56 ± 21.54	162.92 ± 19.55	40.70 ± 4.88
1-6	162	24.27	11.17 ± 1.34	173.64 ± 20.83	124.98 ± 14.99	37.66 ± 4.52

No.of Foil	Thickness (μm)	Energy (MeV)	Activity {(MBq/μAh)/(gm/cm ²)} (m _i)			
			^{nat} Co(p,x) ^{58(m+g)} Co	^{nat} Ni(p,x) ⁵⁷ Ni	^{nat} Mo(p,xn) ^{95g} Tc	^{nat} Mo(p,xn) ^{96(m+g)} Tc
1-9	243	23.29	11.26±1.35	168.04±20.17	148.16±17.78	35.13±4.22
1-12	324	22.27	11.30±1.36	161.55±19.39	130.10±15.61	30.93±3.71
1-15	405	21.22	11.31±1.36	145.88±17.51	127.38±15.28	30.17±3.62
1-18	486	20.12	11.13±1.34	153.33±18.40	127.27±15.27	29.67±3.56
1-21	567	18.98	11.07±1.33	156.09±18.73	136.03±16.32	31.08±3.73
1-24	648	17.79	10.88±1.31	141.83±17.02	147.42±17.69	30.05±3.60
1-27	729	16.53	10.58±1.27	132.14±15.86	142.34±17.08	28.53±3.42
1-30	810	15.12	10.09±1.21	123.23±14.79	125.57±15.07	28.15±3.38
1-33	891	13.77	9.47±1.14	113.80±13.66	125.17±15.02	28.34±3.40
1-36	972	12.23	8.74±1.05	103.74±12.45	128.45±15.41	28.10±3.37
1-39	1053	10.52	8.08±0.97	95.54±11.47	123.75±14.85	30.12±3.61
1-42	1134	8.59	7.52±0.90	89.07±10.69	129.27±15.51	28.60±3.43
1-45	1215	6.28	7.02±0.84	82.70±9.92	112.78±13.53	27.64±3.32
1-48	1296	3.07	6.56±0.79	76.91±9.23	110.45±13.25	25.50±3.06

3.4 Thick target yield of ^{nat}Mo(p,xn)^{95g}Tc

The measured yield as a function of the target thickness for the reaction ^{nat}Mo(p,xn)^{95g}Tc is shown in fig.4. It seen from the figure that, the yield increases gradually with thickness and reaches a saturation value of about 120 MBq/μAh at 110 micron. The contributing reactions to the formation of this isotopes are (p,n), (p,2n) and (p,3n) on different Mo isotopes. An estimated thick target yield values of about 160 and 180 MBq/μAh were given by Bonardi et al.(2002) and Kandahar et al. (2007) respectively. It is clear that our measured value is lower than these estimated by about 25% and 33% respectively. The reason could be attributed to the self-absorption of the measured Gamma rays in the target. The activity due to the production of ⁹⁵Tc isotope per unit surface density in the target (m_i) was calculated from the yield values and found to be about 140 ((MBq/μAh)/(gm/cm²)) over a thickness range from 80 to 1100 micron, as seen in table 5.

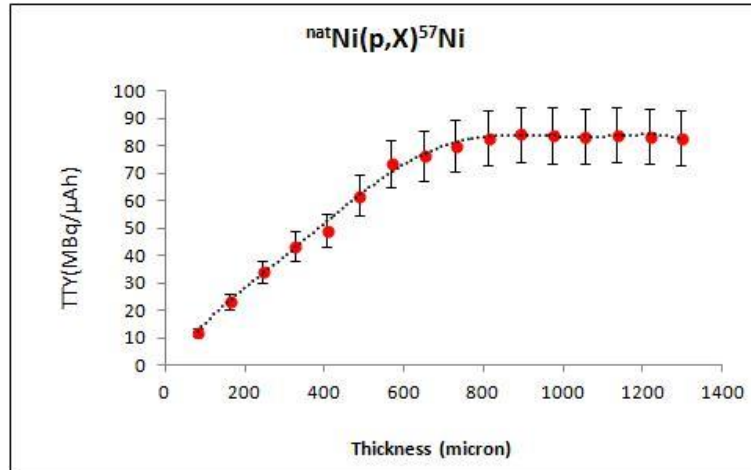


Fig. 3: measured non corrected thick target yield of the nuclear reaction ${}^{\text{nat}}\text{Ni}(p,X){}^{57}\text{Ni}$ as a function of Haver target thickness.

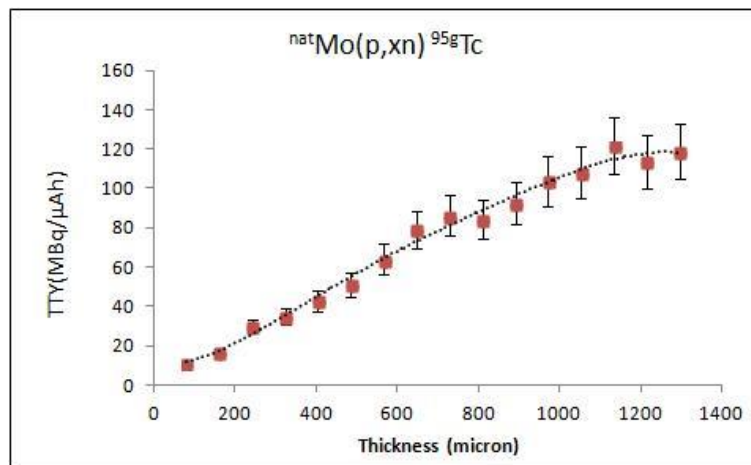


Fig. 4: measured non corrected thick target yield of the nuclear reaction ${}^{\text{nat}}\text{Mo}(p,xn){}^{95g}\text{Tc}$ as a function of Haver target thickness.

3.5. Thick target yield ${}^{\text{nat}}\text{Mo}(p,xn){}^{96(m+g)}\text{Tc}$

Fig.5 shows the results of the measured thick target yield for the reaction ${}^{\text{nat}}\text{Mo}(p,xn){}^{96(m+g)}\text{Tc}$ as a function of the target thickness. The yield value increases linearly with the target thickness and reaches a saturation value of about 30

MBq/μAh at a thickness of 1200 micron. An estimated thick target yield values of about 40 and 36 MBq/μAh were given by Bonardi et al. (2002) and Kandahar et al. (2007) respectively. Our measured value is comparable with the estimated values, within the experimental error. The three reactions (p,n), (p,2n) and (p,3n) on the different Mo isotopes with threshold energies of about 4, 10 and 24.5 MeV respectively, are contributing in the production of $^{96(m+g)}\text{Tc}$. The activity due to the production of $^{96(m+g)}\text{Tc}$ isotope per unit surface density in the target (m_i) was calculated from the yield values and found to about 40 ((MBq/μAh)/(gm/cm²)) in the near surface region and decreases to about 30 ((MBq/μAh)/(gm/cm²)) at about 300 micron, and saturate at this value up to about 1200 micron, as seen in table 5. The higher values at small thickness are due to the large contribution of the (p,3n) reaction. Therefore, the suitable range for using ^{96}Tc for monitoring of Mo is between 300 and 1200 micron.

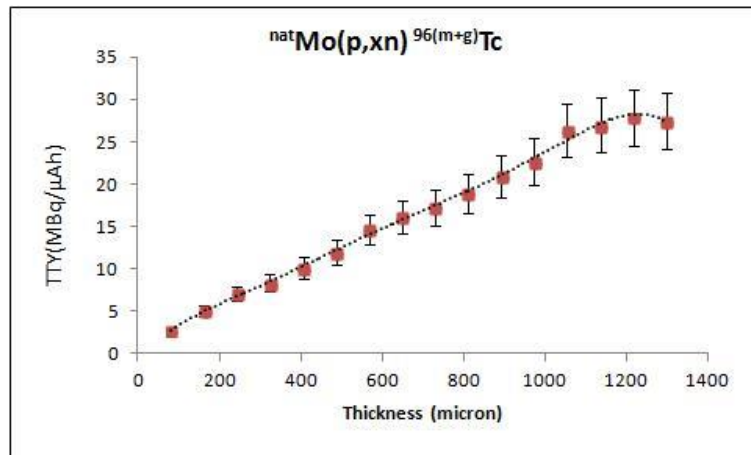


Fig. 5: measured non corrected thick target yield of nuclear reaction $^{nat}\text{Mo}(p,xn)^{96(m+g)}\text{Tc}$ as a function of Haver target thickness.

4. Conclusion

Haver material can be used as a standard material for activation analysis of iron based alloy matrix material, since it contains many elements that could be exist in it, with known certificated concentrations. The stopping power for protons is also very similar in both. Many reactions are given in this work, with their measured yield curves and produced activity per unit surface area's concentration (m_i), can be used for PAA or thin layer activation TLA of steal samples. The yield values, given for these reactions, were experimentally measured and none corrected for self absorption. The results were comparable with some previously estimated values, within the experimental error, sec.(3.3 and 3.4).

References:

- Alharbi, A.A., Alzahrani, J., Azzam, A., 2011. *Radiochim. Acta*, 99, 763-770.
- Al-Saleh, F.S., Al-Harbi, A. A., Azzam, A., 2006. *Radiochim. Acta*, 94, 391-396.
- Barrall, R. C., Merendino, K.A., Nizar Feteih, 1983. *IEEE Transactions on Nuclear Science*, Vol. NS-30, No. 2.
- Bonardi, M., 1988. Report INDC(NDS)-195, p 98. International Atomic Energy Agency.
- Bonardi, M., Birattari, C., Groppi, F. and Sabbioni, E., 2002. *Appl. Radiat. Isot.* 57, 617.
- Cojocaru, V., Badica, T. and Popescu, I. V., 2003. *Romanian Reports in Physics*, 55, 460-463.
- Fireston, R. B., 1998. *Table of Isotopes*, 8th, John Wiley & Sons, United States of America, New York.
- Guerra, M.F., 2004. *Nucl. Instrum. Meth. B* 226, 185.
- Khandaker, M., Uddin, M.S., Kim, K.S., Lee, Y.S., and Kim, G.N., 2007. *Nucl. Instrum. Meth. B* 262, 171.
- Khandaker, M.U., Kim, K.S., Lee, M.W., Kim, K.S., Kim, G.N., 2011. *Nucl. Instrum. Meth. B*, Vol. 269, p. 1140
- Shibata, S., Tanaka, S., Suzuki, T., Umezawa, H., Lot, J. G. and Yeht, S., 1979. *International Journal of Appl. Radiat. Isot.*, 30, 563-565.
- Takacs, S., Tarkanyi, F., Sonck, M., Hermanne, A., 2002. *Nucl. Instrum. Meth. B* 198, 183.
- Titarenko, Yu.E., Batyaev, V.F., Titarenko, A.Yu., Butko, M.A., Pavlov, K.V., S.N.Florya, R.S.Tikhonov, V.M.Zhivun, A.V.Ignatyuk, S.G.Mashnik, S.Leray, A.Boudard, J.Cugnon, D.Mancusi, Y.Yariv, K.Nishihara, N.Matsuda, H.Kumawat, G.Mank, W.Gudowski)
www.nndc.bnl.gov/qcalc/qcalccr.jsp.
- Ziegler, J. F., Biersack, J. P., Littmark, U., 1985: *The Stopping and Range of Ions in Solids*. Vol. 1, Pergamon Press, New York.
- Zweit, J., Carnochan, P., Goodall, R., and Ott, R., J., 1993. *Appl. Radiat. Isot.*, 44, 1411.

تعيين ناتج الهدف السميك لتفاعل البروتونات مع عناصر الموليبدنوم والكوبالت
والنيكل في عينات سبيكة الهيفر Haver للأستخدام التحليلي العنصري
PAA لعينات الصلب

د.أحمد حسن عزام^(١) - د. عبير علي الحربي^(٢) - د. جميله الزهراني^(٢)

١- قسم الطبيعة النووية التجريبية - مركز البحوث النووية - هيئة الطاقة الذرية - القاهرة - مصر

٢- كلية العلوم - جامعة الاميرة نوره بنت عبد الرحمن - الرياض - المملكة العربية السعودية

ملخص البحث. تم قياس ناتج الهدف السميك للتفاعلات النووية ${}^{nat}\text{Ni}(p,x){}^{57}\text{Ni}$, ${}^{nat}\text{Co}(p,x){}^{58(m+g)}\text{Co}$ and ${}^{nat}\text{Mo}(p,x){}^{95g,96(m+g)}\text{Tc}$ كدالة في سمك الهدف باستخدام طريقة تنشيط الشرائح الرقيقة بالبروتونات بطاقة 26.5 MeV. تم استخدام شرائح من سبيكة الهيفر Haver كمادة الهدف حيث أنها تحتوي علي عناصر ${}^{nat}\text{Ni}$, ${}^{nat}\text{Co}$, ${}^{nat}\text{Mo}$ and بتراكيزات دقيقة موثقة. ويمكن استخدام نتائج القياسات في تحليل مكونات عينات الصلب باستخدام طريقة التنشيط بالبروتونات. وتم استخدام سبيكة الهيفر كمرجع نظرا لأنها شديدة الشبه بخصائص سبائك الصلب. وتم ايضا استنتاج قيمة النشاطية الاشعاعية (لأشعة جاما) لنفس الغرض. تمت ايضا مقارنة نتائج القياسات ببعض القيم المقدرة نظريا (مسبقا) في حال توفرها.